
Scaling Sparse Fine-Tuning to Large Language Models

Alan Ansell¹ Ivan Vulić¹ Hannah Sterz¹ Anna Korhonen¹ Edoardo M. Ponti²¹

Abstract

Large Language Models (LLMs) are difficult to fully fine-tune (e.g., with instructions or human feedback) due to their sheer number of parameters. A family of *parameter*-efficient sparse fine-tuning methods have proven promising in terms of performance but their *memory* requirements increase proportionally to the size of the LLMs. In this work, we scale sparse fine-tuning to state-of-the-art LLMs like LLaMA 2 7B and 13B. We propose SpIEL, a novel sparse fine-tuning method which, for a desired density level, maintains an array of parameter indices and the deltas of these parameters relative to their pretrained values. It iterates over: (a) updating the active deltas, (b) pruning indices (based on the change of magnitude of their deltas) and (c) regrowth of indices. For regrowth, we explore two criteria based on either the accumulated gradients of a few candidate parameters or their approximate momenta estimated using the efficient SM3 optimizer. We experiment with instruction-tuning of LLMs on standard dataset mixtures, finding that SpIEL is often superior to popular parameter-efficient fine-tuning methods like LoRA (low-rank adaptation) in terms of performance and comparable in terms of run time. We additionally show that SpIEL is compatible with both quantization and efficient optimizers, to facilitate scaling to ever-larger model sizes. We release the code for SpIEL at <https://github.com/AlanAnsell/peft> and for the instruction-tuning experiments at <https://github.com/ducdauge/sft-llm>.

1. Introduction

The scale of Large Language Models (LLMs), such as Falcon (Almazrouei et al., 2023), LLaMA 2 (Touvron et al., 2023), and Mistral (Jiang et al., 2023), is one of the keys

¹University of Cambridge ²University of Edinburgh. Correspondence to: Alan Ansell <aja63@cam.ac.uk>.

to their state-of-the-art performance (Kaplan et al., 2020). However, this scale is both a blessing and a curse as tailoring LLMs to specific applications via fine-tuning presents a formidable challenge: if performed naïvely, this incurs the cost of updating an incredibly large set of parameters. A family of lightweight methods for LLM adaptation have been proposed to mitigate this issue, known collectively as Parameter-Efficient Fine-Tuning (PEFT). PEFT methods learn a small number of new parameters, denoted as ϕ , which augment the frozen LLM weights θ (Pfeiffer et al., 2023; Lialin et al., 2023). For instance, Low-Rank Adapters (LoRA; Hu et al., 2022) learn additional low-rank matrices to modify the linear layers in Transformer blocks.

PEFT methods based on unstructured sparse fine-tuning (SFT¹), where ϕ is a sparse vector added to θ , have recently shown promise (Sung et al., 2021; Guo et al., 2021; Ansell et al., 2022). These offer a strong trade-off between low number of parameters and high model performance without inserting additional layers into the LLM’s neural architecture, which would reduce model efficiency. In addition, multiple SFTs are *composable* while avoiding interference (Ansell et al., 2022), which facilitates the integration of multiple sources of knowledge into LLMs. Formally, SFT can be conceived of as performing joint optimization over the fixed-size set of non-zero indices of ϕ and their deltas with respect to the LLM weights. Due to the intricacies of this optimization, however, SFT has so far been severely limited by a major drawback, namely, its high memory requirements: existing methods for selecting non-zero indices include learning a mask (Sung et al., 2021), estimating the Fisher information (Guo et al., 2021), or calculating the difference between initialization and convergence (Ansell et al., 2022) for *all LLM parameters*. Hence, SFT is not currently suitable for adapting LLM at large scales.

The main goal of this work is to overcome these challenges by devising memory-efficient methods to update Large Language Models (LLMs) sparsely, while maintaining performance benefits, that is, retaining the same performance of full-model fine-tuning or even surpassing it. Specifically, we wish for the memory use during training (beyond that required to store the pretrained model weights) to scale

¹Note the unfortunate confusion of nomenclature with *supervised* fine-tuning (also frequently referred to as SFT).

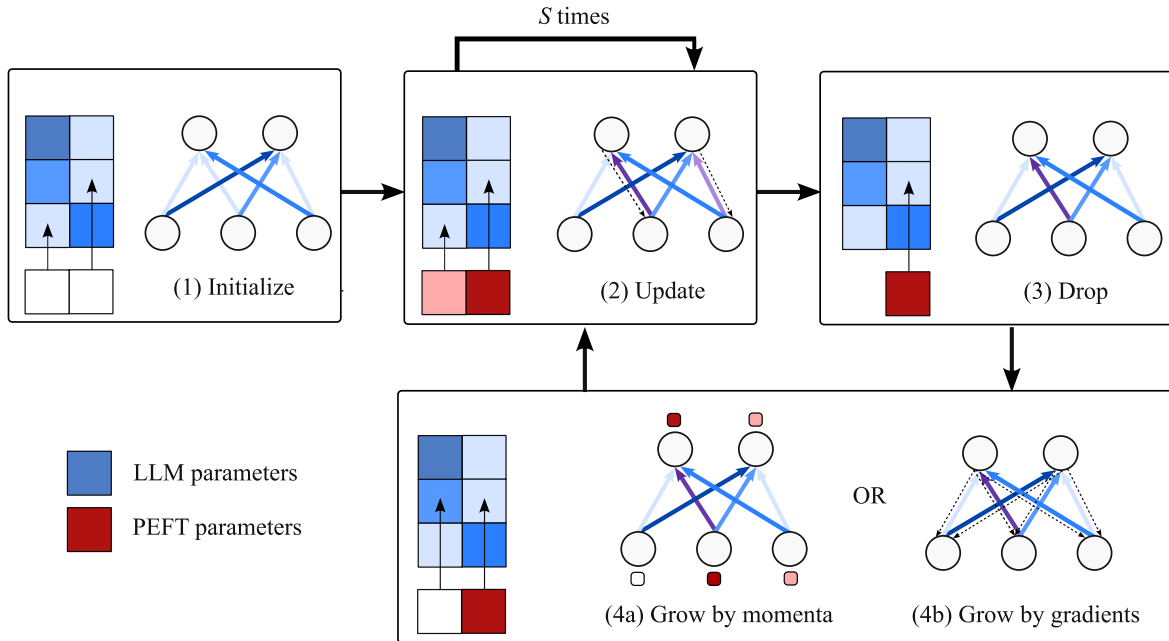


Figure 1. A visualization of the proposed Sparse Fine-Tuning (SFT) method scaled to a Large Language Model (LLM). PEFT parameters consist of indices (arrows) and corresponding deltas (red squares) with respect to LLM parameters (blue squares). After initialization (1), PEFT deltas are updated for S steps (2). Next, obsolete indices are dropped (3) and new indices are grown (4) according to either accumulated gradients or approximate momenta. The algorithm then returns to the update step (2) and is repeated iteratively.

linearly with the number of SFT parameters $\mathcal{O}(d_\phi)$ rather than LLM parameters $\mathcal{O}(d_\theta)$. To achieve this, we introduce SpIEL (Sparse Iterative Efficient Learning), an iterative paradigm for SFT that alternates between updating deltas of active indices, deleting obsolete indices, and growing new ones (Evci et al., 2020). Deletion is determined by change of magnitude between training steps whereas growth by (transiently calculated) gradients. The growth criterion is inspired by Evci et al. (2020), which we further improve upon by *efficiently accumulating* gradients to reduce their variance. Moreover, while our algorithm (SpIEL-AG) is reminiscent of sparse training (Evci et al., 2020), the scattering of the SFT onto the base LLM effectively yields a dense model. This entirely side-steps the problem of the ‘hardware lottery’ due to cumbersome sparse tensor operations (Hooker, 2021). We provide a visual overview of our algorithms in Figure 1.

When extreme memory efficiency is required, we show how SpIEL can be combined with efficient optimizers such as SM3, where the momenta of parameter matrices are approximated by row-wise and column-wise summary metrics (Anil et al., 2019). In these settings, gradients become unreliable, as their variance increases in single-example mini-batches and it is costly memory-wise to accumulate even a subset of them. Hence, we propose that approximate momenta can additionally substitute gradients as a criterion for growth, yielding the SpIEL-MA model variant.

We compare our SpIEL variants with the state-of-the-art PEFT methods LoRA (Hu et al., 2022) and (IA)³ (Liu et al., 2022), as well as with full fine-tuning, starting from LLaMA 2 (Touvron et al., 2023) as a base model. We instruction-tune them on multi-task data such as Flan v2 (Longpre et al., 2023), data generated by proprietary models such as GPT4-Alpaca (Peng et al., 2023), or a mixture of both with Tulu v2 (Iverson et al., 2023). We extensively evaluate the resulting models on standard benchmarks for factuality (MMLU; Hendrycks et al., 2021), reasoning (GSM and BBH; Cobbe et al., 2021; Suzgun et al., 2023), multilinguality (TyDiQA; Clark et al., 2020), and coding (HumanEval; Chen et al., 2021).

The main results reveal that SpIEL outperforms the PEFT and full fine-tuning baselines on most tasks and configurations we test, both with and without 4-bit LLM quantization during fine-tuning (Dettmers et al., 2023). In combination with the SpIEL-MA variant, this allows for scaling fine-tuning to very large LLMs with a modest memory footprint.

2. Background and Related Work

2.1. Parameter-Efficient and Memory-Efficient Fine-Tuning

Parameter-efficient fine-tuning (PEFT) methods have generally been defined as those which fine-tune a small number of parameters relative to the total size of the pretrained

model. The possible benefits of using a PEFT method as opposed to full model fine-tuning include: (1) reduced GPU memory usage during training; (2) faster training; (3) faster saving and loading of the fine-tuning with less permanent storage required as the “frozen” original weights of the large underlying model are shared across multiple tasks and applications; (4) the “composability” property of some PEFT methods, which allows modules to be combined with less interference than with full fine-tuning (Pfeiffer et al., 2020; Ansell et al., 2022); and (5) less tendency to overfit due to the reduced capacity of PEFT with respect to the full model.

Of these, (1) is perhaps the most critical in the era of Large Language Models whose GPU memory requirement for full fine-tuning is beyond the reach of researchers and developers without multiple high-end GPUs. Nonetheless, parameter-efficiency alone does not guarantee a reduction in GPU memory usage, though it almost certainly implies that less space is required to save the fine-tuning in permanent memory. It is thus important to draw a distinction between (i) efficiency in number of fine-tuned parameters versus (ii) the peak GPU memory usage during fine-tuning: we refer to the former as *parameter efficiency* and the latter as *memory efficiency*.

2.2. LoRA

As a solution, Low-Rank Adaptation (LoRA; Hu et al., 2022) is of the best-performing and most popular PEFT techniques to date. In brief, it conceptually fine-tunes only a low-rank subspace of each weight matrix. In practice, LoRA is typically applied only to the linear modules of a Transformer, and is implemented as follows:

$$\mathbf{y} = W\mathbf{x} + \frac{\alpha}{r}BA\mathbf{x}, \quad (1)$$

where $\mathbf{x} \in \mathbb{R}^{d_{\text{in}}}$, $\mathbf{y} \in \mathbb{R}^{d_{\text{out}}}$, $W \in \mathbb{R}^{d_{\text{out}} \times d_{\text{in}}}$, $A \in \mathbb{R}^{r \times d_{\text{in}}}$, $B \in \mathbb{R}^{d_{\text{out}} \times r}$, the subspace rank $r \ll d_{\text{in}}, d_{\text{out}}$, and α is a hyperparameter. Like bottleneck adapters (Houlsby et al., 2019), LoRA employs a successive down- and up-projection, but the fact that it places them in parallel rather than in series with the full-rank matrix multiplication without a non-linearity enables LoRA adapters to be “merged” at inference time into their W matrix as follows:

$$\mathbf{y} = W'\mathbf{x} = (W + \frac{\alpha}{r}BA)\mathbf{x}. \quad (2)$$

This allows LoRA-adapted models to achieve inference speed equal to the underlying LLM.

With the recent development of efficient quantization methods suitable for LLMs, LoRA has emerged as the *de facto* standard PEFT method for LLM instruction tuning (Wang, 2023; Dettmers et al., 2023). This is also why we provide its short self-contained description here and treat it as our principal baseline, while we conduct additional comparisons to (IA)³ (Liu et al., 2022), another established PEFT method.

2.3. Sparse Fine-Tuning

A sparse fine-tuning f' of a neural function f entails the addition of a sparse “difference” or “delta” vector $\delta \in \mathbb{R}^{d_\theta}$ to its parameters $\theta \in \mathbb{R}^{d_\theta}$, i.e. $f'(\cdot; \theta) = f(\cdot; \theta + \delta)$. A delta vector δ with d_ϕ non-zero values can be expressed in terms of a vector of unique indices $\eta \in \{1, 2, \dots, d_\theta\}^{d_\phi}$ and their corresponding values $\phi \in \mathbb{R}^{d_\phi}$. Typically, the SFT density $\frac{d_\phi}{d_\theta}$ is a user-definable hyperparameter. To illustrate the difference between LoRA and SFT visually, Figure 3 shows how they adapt a Transformer block.

In its most general form, sparse fine-tuning can be interpreted as performing joint optimization over η and ϕ :

$$\eta^*, \phi^* = \arg \max_{\eta, \phi} \log p(\mathcal{D} \mid \theta, \eta, \phi). \quad (3)$$

A specialized optimization approach is required for η since it is a discrete latent variable and cannot be directly optimized through stochastic gradient descent. Approaches proposed in previous works include: *DiffPruning* (Guo et al., 2021), which applies a continuous relaxation of a binary mask to δ during fine-tuning which is sparsified with a regularization term, and takes η to be the d_ϕ indices with mask values closest to 1 at the end; *FISH Mask* (Sung et al., 2021), where η is fixed at the beginning of training to be the indices of the d_ϕ weights with highest observed Fisher information; and *Lottery-Ticket SFT* (LT-SFT; Ansell et al., 2022), where η is fixed to be the indices of the d_ϕ weights which change the most during an initial round of full fine-tuning. These methods share a common drawback, namely that the amount of memory they use during training in addition to that required to store the pretrained model weights is proportional to d_θ , the total number of model parameters. As discussed above, this makes these methods prohibitively expensive in many LLM fine-tuning scenarios, especially with very large models; we thus seek a method whose memory overhead is instead proportional to d_ϕ , the number of parameters which are actually modified during fine-tuning.

Finally, there exists a separate but related literature on *pre-training* sparse neural networks, for which we refer the reader to Hoefler et al. (2021) for a detailed overview. This work owes most to Evci et al. (2020), whose dropping and growth paradigm we extend to sparse fine-tuning in §3.2. Contrary to them, however, SPIEL results in a *dense* model, which side-steps the problem that available hardware is not well suited to sparse tensor operations (Hooker, 2021). Moreover, we introduce novel and enhanced growth criteria in Section 3.2 and Section 3.3.

2.4. Quantized PEFT

A significant recent advance in efficient methods for NLP has been the development of quantization methods which are suitable for LLMs and incur minimal degradation in

performance. Dettmers et al. (2022) and later Dettmers et al. (2023) proposed 8-bit and 4-bit quantization techniques for LLM parameter tensors that yield close to full-precision performance during inference or parameter-efficient fine-tuning. The qLoRA fine-tuning method of Dettmers et al. (2023) reduces memory usage by applying 4-bit quantization to most of the pretrained LLM parameters while storing the small number of additional trainable LoRA parameters in full precision and dequantizing the pretrained weights only when required. We show that sparse fine-tuning is also amenable to quantization of the pretrained weights. We use $\text{QUANT}(\cdot)$ and $\text{DEQUANT}(\cdot)$ to denote 4-bit NormalFloat quantization and dequantization respectively with double quantization (Dettmers et al., 2023).

3. Method

3.1. Efficient SFT with Fixed η

In practice, the weights θ of a neural function are partitioned into a sequence of n_p ‘‘parameter tensors.’’ To simplify indexing, we think in terms of the flattened versions of these tensors and refer to them as ‘‘parameter subvectors’’, denoted as $\{\theta^{(1)} \in \mathbb{R}^{d_{\theta^{(1)}}}, \theta^{(2)} \in \mathbb{R}^{d_{\theta^{(2)}}}, \dots, \theta^{(n_p)} \in \mathbb{R}^{d_{\theta^{(n_p)}}}\}$. Similarly, we denote the sections of η and ϕ corresponding to parameter subvector $\theta^{(i)}$ as $\eta^{(i)}$ and $\phi^{(i)}$ respectively. We observe that, for a fixed η and assuming $\max_i d_{\theta^{(i)}} < d_\phi$, it is possible to perform sparse fine-tuning with the desired $\mathcal{O}(d_\phi)$ memory overhead by scatter-adding each $\phi^{(i)}$ into its corresponding $\theta^{(i)}$ (which stays frozen) before it is used:

$$\theta'^{(i)} = \theta^{(i)} + \text{scatter}(\eta^{(i)}, \phi^{(i)}, d_{\theta^{(i)}}), \quad (4)$$

where $\text{scatter}(\eta, \phi, d) \in \mathbb{R}^d$ such that

$$[\text{scatter}(\eta, \phi, d)]_i = \sum_{j=1}^{d_\phi} \mathbb{I}_{\eta_j=i} \phi_j. \quad (5)$$

The simplest way of calculating the gradient of $\phi^{(i)}$ during the backward pass of backpropagation is by gathering the relevant indices of the gradient of $\theta'^{(i)}$:

$$\frac{\partial \mathcal{L}}{\partial \phi_j^{(i)}} = \frac{\partial \mathcal{L}}{\partial \theta_{\eta_j}^{(i)}}. \quad (6)$$

While Equation (6) requires the computation of the dense gradient of each $\theta^{(i)}$, this can be disposed of as soon as the required values are gathered from it. Because $d_{\theta^{(i)}} \ll d_\theta$, this does not add significantly to the peak memory usage. Furthermore, we show in Appendix E that for a linear layer, it is possible in principle to calculate the gradient of $\phi^{(i)}$ without needing to compute the full gradient of $\theta^{(i)}$, which we will explore in future work.

This implementation of sparse fine-tuning stands in contrast to previous approaches (e.g. Sung et al., 2021; Ansell et al.,

2022) which, instead of vectors η and ϕ , maintain a binary mask $\mathbf{b}^{(i)} \in \{0, 1\}^{d_{\theta^{(i)}}$ which is applied to the gradient of $\theta^{(i)}$ after it is calculated. Since \mathbf{b} and the gradient of θ both have size proportional to d_θ , the memory overhead of this implementation is $\mathcal{O}(d_\theta)$. Although the above implementation would enable the fixed- η stage of FISH Mask or LT-SFT to be performed with acceptable memory overhead, both methods incur $\mathcal{O}(d_\theta)$ memory cost when selecting η .

3.2. SpIEL-AG: Accumulated Gradient SpIEL

Building on Evci et al. (2020)’s ‘‘Rigging the Lottery’’ (RigL) method for pretraining sparse neural networks, we propose SpIEL-AG. SpIEL-AG maintains a fixed-size $\eta^{(i)}$ and $\phi^{(i)}$ for each parameter subvector $\theta^{(i)}$, but unlike the methods discussed in the previous section, it allows $\eta^{(i)}$ to change dynamically during training. $\phi^{(i)}$ is initialized as $[0]^{d_{\phi^{(i)}}$ and $\eta^{(i)}$ is initialized as a random subset of $\{1, 2, \dots, d_{\theta^{(i)}}\}$. Every S training steps, $\eta^{(i)}$ is updated by freezing some of the currently trainable weights after resetting them to their pretrained values (‘‘dropping’’), while unfreezing some of the currently frozen weights (‘‘growth’’). A family of possible SpIEL methods arises from the choice of criteria for dropping and growth. For SpIEL-AG, we use the following criteria:

- **DROP**: the $k(i, t)$ weights in $\eta^{(i)}$ which have changed the least from their pretrained values, i.e. $\eta_{\text{drop}}^{(i)} = \text{argtopk}(i, t) - |\phi^{(i)}|$, where $k(i, t)$ is a schedule defining the number of weights in parameter subvector i to replace at step t .
- **GROW**: the $k(i, t)$ weights in $\theta^{(i)}$ with largest estimated ‘‘long-run’’ gradient magnitudes, i.e. $\eta_{\text{grow}}^{(i)} = \text{argtopk}(i, t) \lfloor \mathbb{E}_{\mathbf{x} \sim \mathcal{D}} [\nabla_{\theta^{(i)}} \mathcal{L}(\mathbf{x}; \theta')] \rfloor$.

The gradients required for growth selection are estimated over the γ training steps before η is updated, which we refer to as the *gradient estimation phase*. Here we diverge from Evci et al. (2020), who select the weights to grow on the basis of gradients from a single instantaneous minibatch.³ It is not possible to maintain an estimate of the full gradient of dimension $d_{\theta^{(i)}}$ without exceeding our memory budget. Therefore, we restrict ourselves to maintaining such an estimate for just K_i ‘‘growth candidates.’’ These are selected as the weights in $\theta^{(i)}$ with top K_i gradient magnitudes during the first batch of the gradient estimation phase. The

²The total number of tunable parameters d_ϕ is a hyperparameter, and $d_{\phi^{(i)}}$ is set such that the proportion of tunable parameters $\frac{d_{\phi^{(i)}}}{d_{\theta^{(i)}}$ is the same for each i -th parameter subvector.

³In a memory-constrained setting where it may be possible to process just a single training example at a time, the high level of variance in the gradients from one minibatch may harm the selection of weights to grow.

long-run gradients of the growth candidates are estimated by averaging their gradients over all batches in the gradient estimation phase:

$$\hat{g}_j^{(i)}(t) = \frac{1}{\gamma} \sum_{s=t-\gamma+1}^t \frac{\partial}{\partial \theta_j^{(i)}} \mathcal{L}(\mathbf{x}_s; \boldsymbol{\theta}'). \quad (7)$$

Note that although it is necessary to calculate the dense gradient $\nabla_{\boldsymbol{\theta}^{(i)}} \mathcal{L}(\mathbf{x}; \boldsymbol{\theta}')$ at each step of the gradient estimation phase, we never need to *store* it since we can immediately gather the K_i values we need from it. This can be implemented with a backward hook in PyTorch, for instance. In our experiments, we set $K_i = d_{\phi^{(i)}}$.

There is some additional housekeeping to do after updating $\boldsymbol{\eta}$. We must reset $\phi^{(i)}$ to zero at indices $\text{DROP}(\boldsymbol{\eta}^{(i)})$. We also need to set the optimizer buffers for the newly grown weights $\text{GROW}(\boldsymbol{\eta}^{(i)})$ to appropriate values. In our experiments, we use the Adam optimizer (Kingma & Ba, 2015), which tracks the exponentially smoothed mean of the first and second momenta of the parameter gradients. Conveniently, the gradient estimation phase already produces an estimate of the first momentum of the newly grown weights, and we extend it to estimate the second as well so that we can use these values to seed the optimizer momenta. A minor complication here is that Adam multiplies the i -th momentum by a factor of $\frac{1}{1-\beta_i^t}$ before use to correct for its bias toward zero. Since in SpIEL, different weights are “initialized” at different times, we track the age of each weight (i.e. the number of steps since it was last grown) individually, and use it to calculate the appropriate bias correction.

For simplicity, we set the update rate schedule $k(i, t)$ to decrease linearly to 0 over the course of training, as follows:

$$k(i, t) = \begin{cases} d_{\phi^{(i)}} & \text{if } t = \gamma, \\ \frac{\xi(T-t)}{T} d_{\phi^{(i)}} & \text{otherwise,} \end{cases} \quad (8)$$

where T is the total number of training steps and ξ is a hyperparameter denoting the peak replacement rate. Note that during the first $\boldsymbol{\eta}$ update at step γ , we replace all the weights, since the indices in $\boldsymbol{\eta}$ are randomly initialized; there is no reason to believe that they are relevant to the task.

We provide high-level pseudocode for SpIEL-AG in Algorithm 1. Note that some details such as the selection of candidates and optimizer momenta seeding are omitted for conciseness.

3.3. SpIEL-MA: Momentum-Approximation SpIEL

The SpIEL-AG method prioritizes making a high-quality selection of weights to grow when updating $\boldsymbol{\eta}$, but this comes at the cost of the extra memory required during the gradient estimation phase to store the indices of the growth candi-

Algorithm 1 Accumulated Gradient SpIEL

```

1: procedure SpIEL-AG( $\boldsymbol{\theta}, \mathcal{D}, \gamma, k$ )
2:    $\phi \leftarrow [0]^{d_\phi}$  ▷ Initialize SFT values
3:    $\phi_0 \leftarrow \phi$ 
4:    $\boldsymbol{\eta} \sim_{d_\phi} [1..d_\theta]$  ▷ Initialize SFT indices
5:   for  $t$  in  $1..T$  do
6:      $\mathbf{x}_t \sim \mathcal{D}$ 
7:      $\boldsymbol{\theta}' \leftarrow \text{scatter-add}(\phi, \boldsymbol{\eta}, \boldsymbol{\theta})$ 
8:     UPDATE( $\phi, \nabla_\phi \mathcal{L}(f_{\boldsymbol{\theta}'}(\mathbf{x}_t))$ )
9:     if  $\gamma | t$  then
10:       $\mathbf{d} \leftarrow \text{top-}k(t)(-|\phi - \phi_0|)$ 
11:       $\phi, \boldsymbol{\eta} = \text{DROP}(\phi, \boldsymbol{\eta}, \mathbf{d})$ 
12:       $\mathbf{g} \leftarrow \text{top-}k(t)[\sum_{i=t-\gamma+1}^t \nabla_{\boldsymbol{\theta}} \mathcal{L}(f_{\boldsymbol{\theta}'}(\mathbf{x}_i))]$ 
13:       $\phi, \boldsymbol{\eta} = \text{GROW}(\phi, \boldsymbol{\eta}, \mathbf{g})$ 
14:       $\phi_0 \leftarrow \phi$ 
15:   return  $\phi, \boldsymbol{\eta}$ 

```

dates and their estimated momenta. We propose an alternative algorithm for the most memory-constrained scenarios, which we call SpIEL-MA, employing the SM3 memory-efficient adaptive optimizer of Anil et al. (2019). For a two-dimensional parameter tensor Θ of size $r \times c$, the SM3 optimizer maintains buffers $\mathbf{r} \in \mathbb{R}^r$ and $\mathbf{c} \in \mathbb{R}^c$, which contain running sums of the maximum squared gradients over the columns and rows of Θ , respectively. We can obtain a (low-quality but cheap) estimate of the absolute value of the momentum m_{ij} for each element θ_{ij} of Θ by taking the elementwise fourth root of the outer product of \mathbf{r} and \mathbf{c} :

$$|\hat{m}|_{ij} = \sqrt[4]{r_i c_j}. \quad (9)$$

SpIEL-MA uses this estimate to rank weights for growth, and otherwise it is the same as SpIEL-AG. Since the SM3 optimizer is very memory efficient, storing only $r+c$ values in its buffers for an $r \times c$ parameter tensor compared to Adam’s $2rc$, and SpIEL-MA uses no additional persistent memory to track statistics to inform $\boldsymbol{\eta}$ updates, significantly less memory in total is required than for SpIEL-AG. Incidentally, we remark that the growth criterion of SpIEL-MA assumes **locality**, i.e., that the importance of a parameter is correlated to those in the same row and column. This is reminiscent of the locality-driven synaptic growth in human brains, which results in dense hubs but a globally sparse anatomy (Betz et al., 2017; Hoefler et al., 2021). We provide high-level pseudocode for SpIEL-MA in Algorithm 2.

Regularizing SpIEL Similar to LoRA, which is regularized by its dropout, SpIEL is also likely to overfit as the model diverges from its pretrained state. We therefore regularize SpIEL by applying L2 regularization to the ϕ parameters in the form of weight decay with strength λ .

Quantized SpIEL As another contribution, we extend the

Algorithm 2 Momentum-Approximation SpIEL

```

1: procedure SpIEL-MA( $\theta^{(1)}, \dots, \theta^{(n_p)}, \mathcal{D}, \gamma, k$ )
2:   for  $i$  in  $1..P$  do
3:      $\phi^{(i)} \leftarrow [0]^{d_{\phi^{(i)}}$ 
4:      $\phi_0^{(i)} \leftarrow \phi^{(i)}$ 
5:      $\eta^{(i)} \sim_{d_{\phi^{(i)}}} [1..d_{\theta^{(i)}}]$ 
6:      $\mathbf{r}^{(i)} = [0]^{h^{(i)}} \triangleright$  Initialize row accumulator
7:      $\mathbf{c}^{(i)} = [0]^{w^{(i)}} \triangleright$  Initialize column accumulator
8:   for  $t$  in  $1..T$  do
9:      $\mathbf{x} \sim \mathcal{D}$ 
10:     $\theta' \leftarrow \text{concat}_i \text{scatter-add}(\phi^{(i)}, \eta^{(i)}, \theta^{(i)})$ 
11:    for  $i$  in  $1..n_p$  do
12:      UPDATE-SM3[ $\phi^{(i)}, \eta^{(i)}, \mathbf{r}^{(i)}, \mathbf{c}^{(i)}$ ,
13:         $\nabla_{\phi^{(i)}} \mathcal{L}(f_{\theta'}(\mathbf{x}))]$ 
14:      if  $\gamma | t$  then
15:         $\mathbf{d}^{(i)} \leftarrow \text{top-}k(i, t)(-\|\phi^{(i)} - \phi_0^{(i)}\|)$ 
16:         $\phi^{(i)}, \eta^{(i)} = \text{DROP}(\phi^{(i)}, \eta^{(i)}, \mathbf{d}^{(i)})$ 
17:         $\mathbf{g}^{(i)} \leftarrow \text{top-}k(i, t)[\mathbf{r}^{(i)} \otimes \mathbf{c}^{(i)}]$ 
18:         $\phi^{(i)}, \eta^{(i)} = \text{GROW}(\phi^{(i)}, \eta^{(i)}, \mathbf{g}^{(i)})$ 
19:         $\phi_0^{(i)} \leftarrow \phi^{(i)}$ 
20:    return  $\phi^{(1)}, \dots, \phi^{(n_p)}, \eta^{(1)}, \dots, \eta^{(n_p)}$ 

```

proposed SpIEL techniques to quantized LLMs (“qSpIEL”). Consider parameter matrix $W_{\text{PT}}^{(i)} \in \mathbb{R}^{h \times o}$ in its pre-trained data type (e.g., FP32). Instead of storing $W_{\text{PT}}^{(i)}$ itself on GPU, we store its quantized version $W_{\text{NF4}}^{(i)} = \text{QUANT}(W_{\text{PT}}^{(i)})$. During the forward pass of the linear module, qSpIEL computes the following:

$$Y = X(\text{DEQUANT}(W_{\text{PT}}^{(i)}) + \Delta W^{(i)}), \quad (10)$$

where $X \in \mathbb{R}^{b \times h}$ is the input to the linear module, $Y \in \mathbb{R}^{b \times o}$ is the output, and

$$\Delta W^{(i)} = \text{reshape}(\text{scatter}(\eta^{(i)}, \phi^{(i)}, h_o), [h, o]).$$

This is equivalent to the behavior of a linear module in ordinary, non-quantized SpIEL except that the pretrained parameter matrix gets quantized at the beginning of training and temporarily dequantized each time it is used.

4. Experimental Setup

4.1. Training and Evaluation Data

To demonstrate the effectiveness of SpIEL, we loosely base our experimental setup on that of Wang et al. (2023), who compare different data mixtures. In particular, we instruction-tune LLMs on (i) Wang et al. (2023)’s 50K subsample of Flan v2 (Longpre et al., 2023), a dataset collecting manually annotated examples for multiple tasks augmented with instructions; (ii) GPT4-Alpaca (Peng et al., 2023), a

dataset of 50K outputs generated by davinci-003 and GPT-4 (OpenAI, 2023) prompted with inputs from Alpaca (Taori et al., 2023); or (iii) the Tülu v2 mixture (Iverson et al., 2023), consisting of 326K examples from multiple instruction following datasets.

Following Wang et al. (2023) and Iverson et al. (2023), we evaluate instruction-tuned LLMs on the following benchmarks to capture a range of abilities: Massively Multitask Language Understanding (MMLU; Hendrycks et al., 2021), Grade School Math (GSM; Cobbe et al., 2021), BIG-Bench Hard (BBH; Suzgun et al., 2023), Typologically Diverse Question Answering (TyDiQA; Clark et al., 2020) and HumanEval (Chen et al., 2021). We report combinations of training data mixtures and downstream evaluation benchmarks where Wang et al. (2023) reports the highest gains. See Appendix B for full details of our evaluation setup.

4.2. Models and Baselines

As LLMs to fine-tune, we choose state-of-the-art LLaMA 2 (Touvron et al., 2023) at both 7b and 13b parameter scales. We report the performance of the unmodified “vanilla” models as a baseline for a series of PEFT methods. Specifically, we compare SpIEL with LoRA (Hu et al., 2022, see §2.2), as it offers the best performance–efficiency trade-off (Pfeiffer et al., 2023) and is arguably the most widespread pre-existing PEFT method (Detmers et al., 2023), as well as (IA)³ (Liu et al., 2022). We use the LoRA and (IA)³ implementations in the peft library (Mangrulkar et al., 2022). For the Tülu v2 fine-tuning mixture, we include the fully fine-tuned LLaMA 2 models of Iverson et al. (2023) as a baseline (“FullIFT”), which we would expect to provide a soft upper bound on the performance of the PEFT methods.⁴ At 7b scale, we also perform our own full fine-tuning on the Flan v2 and GPT4-Alpaca splits. We did not perform these experiments at 13b scale due to the computational expense.

Note that the pre-existing SFT methods (see §2.3) such as DiffPruning (Sung et al., 2021), FISH Mask (Guo et al., 2021), and LT-SFT (Ansell et al., 2022) are not viable as baselines for LLM fine-tuning as their memory complexity scales as $\mathcal{O}(d_{\theta})$, similar to full fine-tuning. Full details of the training setup and hyperparameters can be found in Appendix C.

5. Results

5.1. Main Results

We present the main results of our experiments in Table 1. For Llama2-7b, we find that SpIEL-AG outperforms LoRA and (IA)³ consistently across evaluation benchmarks and in-

⁴These follow a similar hyper-parameter setup except for a much higher maximum context length of 8,192.

Table 1. Performance of PEFT methods on a range of evaluation tasks for various instruction tuning datasets. † indicates results obtained using the models of Ivison et al. (2023). Tülu v2 \oplus GPT4-Alpaca refers to a setting where we compose the respective PEFTs.

		Flan v2		GPT4-Alpaca	Tülu v2				Tülu v2 \oplus GPT4-Alpaca	
Model / Method		MMLU	TyDiQA	HumanEval	MMLU	GSM	BBH	TyDiQA	HumanEval	HumanEval
Llama2-7b	Original	45.8	50.9	13.5	45.8	13.0	40.6	50.9	13.5	-
	FullIFT	50.5	55.5	15.2	51.3 [†]	34.5 [†]	45.3 [†]	56.5 [†]	22.6 [†]	-
	(IA) ³	46.7	51.6	14.7	47.8	17.0	40.6	52.2	15.5	16.6
	LoRA	49.3	55.3	15.7	51.3	22.0	43.8	58.0	15.5	16.1
	SpIEL-AG	50.7	56.2	15.6	51.5	23.0	44.8	59.4	17.1	18.8
	SpIEL-MA	48.8	55.8	16.2	49.5	16.5	44.7	56.7	15.3	17.0
Llama2-13b	Original	55.3	60.3	17.8	55.3	23.0	47.8	60.3	17.8	-
	FullIFT	-	-	-	56.7 [†]	50.0 [†]	51.9 [†]	62.9 [†]	26.7 [†]	-
	(IA) ³	55.1	60.1	18.5	55.6	27.5	50.6	62.8	18.1	18.4
	LoRA	55.8	61.4	19.8	56.2	29.0	54.6	63.9	19.5	22.4
	SpIEL-AG	55.8	62.5	20.0	55.9	31.5	52.8	63.5	20.3	22.7
	SpIEL-MA	55.5	62.5	19.9	55.9	29.0	51.2	62.8	20.2	20.8

Table 2. Performance of quantized PEFT methods on a range of evaluation tasks for various instruction tuning datasets.

		Flan v2		GPT4-Alpaca
Model / Method		MMLU	TyDiQA	HumanEval
L12-7b	Original (4-bit)	44.8	50.2	11.0
	qLoRA	47.7	54.3	13.3
	qSpIEL-AG	48.8	54.9	15.3
	qSpIEL-MA	48.3	52.7	15.3
L12-13b	Original (4-bit)	54.7	59.6	15.5
	qLoRA	55.0	60.7	18.2
	qSpIEL-AG	55.5	61.5	18.8
	qSpIEL-MA	55.4	61.7	18.4

struction tuning datasets, including Flan v2, GPT4-Alpaca, and Tülu v2. For Llama2-13b, SpIEL-AG similarly outperforms all baselines when fine-tuned on Flan v2 and GPT4-Alpaca; however, we report more mixed results for Tülu v2.⁵ Nonetheless, SpIEL-AG is superior in 5 out of the 6 combinations of scales and instruction tuning datasets. Hence, SpIEL-AG appears to be the strongest method overall.

AG vs MA Comparing the two SpIEL growth criteria, there appears to be a trade-off between performance and memory usage, with the more memory-efficient SpIEL-MA generally performing a little worse than SpIEL-AG, except for a few cases, such as HumanEval evaluation for Llama2-7b. Since GPT4-Alpaca (used for HumanEval evaluation) has the same amount of training examples as Flan v2, we rule out that this difference is due to different levels of sample efficiency between SpIEL-AG and SpIEL-MA.

Ceiling We find that SpIEL-AG generally matches the per-

⁵It is possible that the hyperparameters chosen for SpIEL during the hyperparameter search on Flan v2 do not always transfer well to Tülu v2, which is a much larger dataset with a different distribution of task types.

formance of full fine-tuning on most tasks, except GSM and HumanEval when fine-tuned on Tülu v2, where FullIFT vastly outperforms all PEFT methods. This effect was also observed by Ivison et al. (2023) in their qLoRA evaluation. We note that the maximum sequence length we use during fine-tuning is 2,048, whereas Ivison et al. (2023) use 8,192 for full fine-tuning and 4,096 for qLoRA. It is possible that the shorter sequence length for PEFT has a significant effect on downstream performance for open-ended generation tasks, or that PEFT is weaker on these tasks in general, perhaps due to its inability to modify the input and output embedding layers. This warrants further investigation as part of future work.

Quantization According to the scores in Table 2, we find that 4-bit quantization results in only a modest reduction in performance across PEFT methods, and their relative performance remains similar. In fact, SpIEL-AG is superior again to both LoRA and (IA)³ by an even higher margin compared to Table 1. These results demonstrate that SpIEL is a competitive PEFT method even in extremely resource-constrained scenarios.

Compositionality Finally, in Table 1 we also study whether *multiple* PEFT adapters, trained on different data mixtures, can be composed with the LLM. We find that composing GPT4-Alpaca and Tülu v2 adapters increases the performance on HumanEval for PEFT, compared to the individual adapters. However SpIEL-AG performs favorably in composition compared to LoRA as it yields a larger boost for 7B (+1.7 vs +0.4) and an overall better performance on 13B.

5.2. Training Speed and Memory Efficiency

In Table 3, we compare the memory requirements and training time of LoRA, SpIEL and their quantized variants. We consider two settings, with and without activation check-

Table 3. GPU memory requirements (in GB) and average time per training step (in seconds) for fine-tuning SFT and LoRA on Flan v2 on an A100 GPU. We report values either without (left) or with (right) activation checkpointing.

Method	LLaMA 2 7b		LLaMA 2 13b	
	Mem. ↓	Time ↓	Mem. ↓	Time ↓
LoRA	40 / 18	30.5 / 42.5	66 / 31	45.9 / 64.0
SpIEL-AG	34 / 20	33.4 / 44.8	56 / 36	56.2 / 76.3
SpIEL-MA	30 / 17	30.6 / 41.7	51 / 31	50.6 / 70.9
qLoRA	30 / 8	38.5 / 55.2	46 / 12	63.6 / 95.3
qSpIEL-AG	26 / 13	42.8 / 58.4	40 / 19	73.4 / 101.1
qSpIEL-MA	22 / 10	39.6 / 55.5	35 / 14	70.1 / 97.3

pointing.⁶ We define the memory requirements to be the minimum amount of GPU memory needed to complete training successfully. We provide more details on our measurements in Appendix F.

We find that LoRA, SpIEL-AG and SpIEL-MA are broadly similar in terms of speed and memory requirements. SpIEL-MA is consistently somewhat faster and more memory efficient than SpIEL-AG. Without activation checkpointing, we find that the SpIEL methods are more memory efficient than LoRA; however, activation checkpointing is especially effective in reducing LoRA’s memory consumption, likely because LoRA stores more intermediate activations due to the parallel computation of the LoRA update. When both quantization and activation checkpointing are applied, LoRA is the most memory-efficient technique by a small margin.⁷ We also find that LoRA is generally slightly faster than the SpIEL methods, despite being generally outperformed by SpIEL-AG, especially with quantization.

As expected, quantization and activation checkpointing both trade a slowdown in training speed for a reduction in memory usage. However, as a more general finding, these results would suggest that activation checkpointing should be prioritized ahead of quantization in most cases when performing PEFT on LLMs of this size (≥ 7 B), as a larger memory saving is achieved for an only marginally larger slowdown, and without incurring any cost in performance.

5.3. Parameter Ages

To shed light on the training dynamics of SpIEL, we study the age of each index (i.e., the iteration when it was last grown) of the converged parameters. We plot the proportion

⁶Note that “activation checkpointing” is a synonym of “gradient checkpointing”.

⁷We note that, unlike our qSpIEL implementation, qLoRA employs a paged optimizer, which might explain why there is a larger memory reduction for qLoRA. While qSpIEL is also compatible with the use of paged optimizers, we leave the actual implementation for future work.

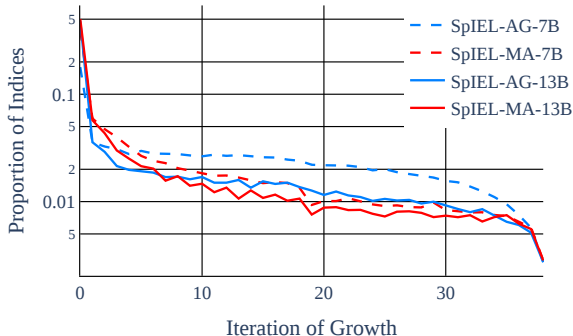


Figure 2. Proportion of indices with a certain age (i.e., the iteration when they were last grown) of the converged η after training on the Flan v2 dataset.

of indices grown at a certain iteration in Figure 2, based on models trained on Flan v2. In general, SpIEL-MA introduces fewer new parameter indices later in training compared to SpIEL-AG. We also find that 13b models tend to retain parameter indices found earlier in training compared to their 7b counterparts. This preference for earlier index sets is not necessarily desirable as it might reflect the fact that SpIEL-MA and 13b models tend to get stuck in early local minima. We speculate that better schedules for dropping and growth might alleviate this issue in the future.

6. Conclusions and Future Work

We have proposed SpIEL, the first method (to our knowledge) for Sparse Fine-Tuning (SFT) that is not only parameter-efficient but also memory-efficient. This allows it to scale to Large Language Models. Taking inspiration from iterative methods for sparse pre-training, we alternate among phases where we update, drop, and then grow parameters. In particular, we introduce two new criteria for parameter growth: Accumulated Gradients across multiple iterations (SpIEL-AG) and Momentum Approximation (SpIEL-MA), where we reuse information tracked by optimizers like SM3. We find that SpIEL often surpasses alternative PEFT methods such as (IA)³ and LoRA in terms of performance and is comparable to them in terms of memory and time efficiency.

We hope that these promising results will encourage further research into sparse fine-tuning. Future work may include extending SpIEL to the embedding layers of LLMs; improving the efficiency of the backward pass for a linear layer (see Appendix E); considering more advanced dropping/growth criteria, especially those which would enable adaptive redistribution of tunable parameters across parameters tensors. This would stand in contrast to the current setup where the number of tunable parameters in each tensor is fixed.

Acknowledgments

Alan Ansell wishes to thank David and Claudia Harding for their generous support via the Harding Distinguished Postgraduate Scholarship Programme. This work has been in part supported by the UK Research and Innovation (UKRI) Frontier Research Grant EP/Y031350/1 (the UK government’s funding guarantee for ERC Advanced Grants) awarded to Anna Korhonen. Ivan Vulić has also been supported by a personal Royal Society University Research Fellowship ‘*Inclusive and Sustainable Language Technology for a Truly Multilingual World*’ (no 221137; 2022-). Hannah Sterz thanks the Cambridge Trust for their support via the International Scholarship.

References

- Almazrouei, E., Alobeidli, H., Alshamsi, A., Cappelli, A., Cojocar, R., Debbah, M., Goffinet, E., Heslow, D., Lounay, J., Malartic, Q., Noune, B., Pannier, B., and Penedo, G. Falcon-40B: An open large language model with state-of-the-art performance. Technical report, Technology Innovation Institute, 2023.
- Anil, R., Gupta, V., Koren, T., and Singer, Y. Memory-efficient adaptive optimization. In *Proceedings of the 33rd International Conference on Neural Information Processing Systems*, Red Hook, NY, USA, 2019.
- Ansell, A., Ponti, E., Korhonen, A., and Vulić, I. Composable sparse fine-tuning for cross-lingual transfer. In *Proceedings of the 60th Annual Meeting of the Association for Computational Linguistics (Volume 1: Long Papers)*, pp. 1778–1796, Dublin, Ireland, May 2022.
- Betzel, R. F., Medaglia, J. D., Papadopoulos, L., Baum, G. L., Gur, R., Gur, R., Roalf, D., Satterthwaite, T. D., and Bassett, D. S. The modular organization of human anatomical brain networks: Accounting for the cost of wiring. *Network Neuroscience*, 1(1):42–68, 2017.
- Chen, M., Tworek, J., Jun, H., Yuan, Q., de Oliveira Pinto, H. P., Kaplan, J., Edwards, H., Burda, Y., Joseph, N., Brockman, G., Ray, A., Puri, R., Krueger, G., Petrov, M., Khlaaf, H., Sastry, G., Mishkin, P., Chan, B., Gray, S., Ryder, N., Pavlov, M., Power, A., Kaiser, L., Bavarian, M., Winter, C., Tillet, P., Such, F. P., Cummings, D., Plappert, M., Chantzis, F., Barnes, E., Herbert-Voss, A., Guss, W. H., Nichol, A., Paino, A., Tezak, N., Tang, J., Babuschkin, I., Balaji, S., Jain, S., Saunders, W., Hesse, C., Carr, A. N., Leike, J., Achiam, J., Misra, V., Morikawa, E., Radford, A., Knight, M., Brundage, M., Murati, M., Mayer, K., Welinder, P., McGrew, B., Amodei, D., McCandlish, S., Sutskever, I., and Zaremba, W. Evaluating large language models trained on code. *arXiv preprint arXiv:2107.03374*, 2021.
- Clark, J. H., Choi, E., Collins, M., Garrette, D., Kwiatkowski, T., Nikolaev, V., and Palomaki, J. TyDi QA: A benchmark for information-seeking question answering in typologically diverse languages. *Transactions of the Association for Computational Linguistics*, 8:454–470, 2020.
- Cobbe, K., Kosaraju, V., Bavarian, M., Chen, M., Jun, H., Kaiser, L., Plappert, M., Tworek, J., Hilton, J., Nakano, R., Hesse, C., and Schulman, J. Training verifiers to solve math word problems. *arXiv preprint arXiv:2110.14168*, 2021.
- Dettmers, T., Lewis, M., Belkada, Y., and Zettlemoyer, L. GPT3.int8(): 8-bit matrix multiplication for transformers at scale. In *Advances in Neural Information Processing Systems 35: Annual Conference on Neural Information Processing Systems 2022, NeurIPS 2022, New Orleans, LA, USA, November 28 - December 9, 2022*.
- Dettmers, T., Pagnoni, A., Holtzman, A., and Zettlemoyer, L. QLoRA: Efficient finetuning of quantized LLMs. *arXiv preprint arXiv:2305.14314*, 2023.
- Evcı, U., Gale, T., Menick, J., Castro, P. S., and Elsen, E. Rigging the lottery: Making all tickets winners. In III, H. D. and Singh, A. (eds.), *Proceedings of the 37th International Conference on Machine Learning*, volume 119 of *Proceedings of Machine Learning Research*, pp. 2943–2952, 13–18 Jul 2020.
- Guo, D., Rush, A., and Kim, Y. Parameter-efficient transfer learning with diff pruning. In *Proceedings of the 59th Annual Meeting of the Association for Computational Linguistics and the 11th International Joint Conference on Natural Language Processing (Volume 1: Long Papers)*, pp. 4884–4896, Online, August 2021.
- Hendrycks, D., Burns, C., Basart, S., Zou, A., Mazeika, M., Song, D., and Steinhardt, J. Measuring massive multitask language understanding. In *International Conference on Learning Representations*, 2021.
- Hoefler, T., Alistarh, D., Ben-Nun, T., Dryden, N., and Peste, A. Sparsity in deep learning: Pruning and growth for efficient inference and training in neural networks. *The Journal of Machine Learning Research*, 22(1):10882–11005, 2021.
- Hooker, S. The hardware lottery. *Communications of the ACM*, 64(12):58–65, 2021.
- Houlsby, N., Giurgiu, A., Jastrzebski, S., Morrone, B., De Laroussilhe, Q., Gesmundo, A., Attariyan, M., and Gelly, S. Parameter-efficient transfer learning for NLP. In Chaudhuri, K. and Salakhutdinov, R. (eds.), *Proceedings of the 36th International Conference on Machine Learning*

- Learning*, volume 97 of *Proceedings of Machine Learning Research*, pp. 2790–2799, 09–15 Jun 2019.
- Hu, E. J., yelong shen, Wallis, P., Allen-Zhu, Z., Li, Y., Wang, S., Wang, L., and Chen, W. LoRA: Low-rank adaptation of large language models. In *International Conference on Learning Representations*, 2022.
- Iverson, H., Wang, Y., Pyatkin, V., Lambert, N., Peters, M., Dasigi, P., Jang, J., Wadden, D., Smith, N. A., Beltagy, I., and Hajishirzi, H. Camels in a changing climate: Enhancing LM adaptation with Tulu 2. *arXiv preprint arXiv:2311.10702*, abs/2311.10702, 2023.
- Jiang, A. Q., Sablayrolles, A., Mensch, A., Bamford, C., Chaplot, D. S., de las Casas, D., Bressand, F., Lengyel, G., Lample, G., Saulnier, L., Lavaud, L. R., Lachaux, M.-A., Stock, P., Scao, T. L., Lavril, T., Wang, T., Lacroix, T., and Sayed, W. E. Mistral 7B. *arXiv preprint arXiv:2310.06825*, 2023.
- Kaplan, J., McCandlish, S., Henighan, T., Brown, T. B., Chess, B., Child, R., Gray, S., Radford, A., Wu, J., and Amodei, D. Scaling laws for neural language models. *arXiv preprint arXiv:2001.08361*, 2020.
- Kingma, D. P. and Ba, J. Adam: A method for stochastic optimization. In Bengio, Y. and LeCun, Y. (eds.), *3rd International Conference on Learning Representations, ICLR 2015, San Diego, CA, USA, May 7-9, 2015, Conference Track Proceedings*, 2015.
- Lialin, V., Deshpande, V., and Rumshisky, A. Scaling down to scale up: A guide to parameter-efficient fine-tuning. *arXiv preprint arXiv:2303.15647*, 2023.
- Liu, H., Tam, D., Muqeeth, M., Mohta, J., Huang, T., Bansal, M., and Raffel, C. A. Few-shot parameter-efficient fine-tuning is better and cheaper than in-context learning. In Koyejo, S., Mohamed, S., Agarwal, A., Belgrave, D., Cho, K., and Oh, A. (eds.), *Advances in Neural Information Processing Systems*, volume 35, pp. 1950–1965, 2022.
- Longpre, S., Hou, L., Vu, T., Webson, A., Chung, H. W., Tay, Y., Zhou, D., Le, Q. V., Zoph, B., Wei, J., and Roberts, A. The flan collection: Designing data and methods for effective instruction tuning. In Krause, A., Brunskill, E., Cho, K., Engelhardt, B., Sabato, S., and Scarlett, J. (eds.), *International Conference on Machine Learning, ICML 2023, 23-29 July 2023, Honolulu, Hawaii, USA*, volume 202 of *Proceedings of Machine Learning Research*, pp. 22631–22648, 2023.
- Mangrulkar, S., Gugger, S., Debut, L., Belkada, Y., and Paul, S. Peft: State-of-the-art parameter-efficient fine-tuning methods. <https://github.com/huggingface/peft>, 2022.
- OpenAI. GPT-4 technical report. *arXiv preprint arXiv:2303.08774*, 2023.
- Peng, B., Li, C., He, P., Galley, M., and Gao, J. Instruction tuning with GPT-4. *arXiv preprint arXiv:2304.03277*, 2023.
- Pfeiffer, J., Vulić, I., Gurevych, I., and Ruder, S. MAD-X: An Adapter-Based Framework for Multi-Task Cross-Lingual Transfer. In *Proceedings of the 2020 Conference on Empirical Methods in Natural Language Processing (EMNLP)*, pp. 7654–7673, Online, November 2020.
- Pfeiffer, J., Ruder, S., Vulić, I., and Ponti, E. Modular deep learning. *Transactions on Machine Learning Research*, 2023.
- Sung, Y.-L., Nair, V., and Raffel, C. A. Training neural networks with fixed sparse masks. In Ranzato, M., Beygelzimer, A., Dauphin, Y., Liang, P., and Vaughan, J. W. (eds.), *Advances in Neural Information Processing Systems*, volume 34, pp. 24193–24205, 2021.
- Suzgun, M., Scales, N., Schärli, N., Gehrmann, S., Tay, Y., Chung, H. W., Chowdhery, A., Le, Q. V., Chi, E., Zhou, D., and Wei, J. Challenging big-bench tasks and whether chain-of-thought can solve them. In Rogers, A., Boyd-Graber, J. L., and Okazaki, N. (eds.), *Findings of the Association for Computational Linguistics: ACL 2023, Toronto, Canada, July 9-14, 2023*, pp. 13003–13051, 2023.
- Taori, R., Gulrajani, I., Zhang, T., Dubois, Y., Li, X., Guestrin, C., Liang, P., and Hashimoto, T. B. Stanford Alpaca: An instruction-following LLaMA model. https://github.com/tatsu-lab/stanford_alpaca, 2023.
- Touvron, H., Martin, L., Stone, K., Albert, P., Almahairi, A., Babaei, Y., Bashlykov, N., Batra, S., Bhargava, P., Bhosale, S., Bikel, D., Blecher, L., Ferrer, C. C., Chen, M., Cucurull, G., Esiobu, D., Fernandes, J., Fu, J., Fu, W., Fuller, B., Gao, C., Goswami, V., Goyal, N., Hartshorn, A., Hosseini, S., Hou, R., Inan, H., Kardas, M., Kerkez, V., Khabsa, M., Kloumann, I., Korenev, A., Koura, P. S., Lachaux, M.-A., Lavril, T., Lee, J., Liskovich, D., Lu, Y., Mao, Y., Martinet, X., Mihaylov, T., Mishra, P., Molybog, I., Nie, Y., Poulton, A., Reizenstein, J., Rungta, R., Saladi, K., Schelten, A., Silva, R., Smith, E. M., Subramanian, R., Tan, X. E., Tang, B., Taylor, R., Williams, A., Kuan, J. X., Xu, P., Yan, Z., Zarov, I., Zhang, Y., Fan, A., Kambadur, M., Narang, S., Rodriguez, A., Stojnic, R., Edunov, S., and Scialom, T. Llama 2: Open foundation and fine-tuned chat models. *arXiv preprint arXiv:2307.09288*, 2023.
- Wang, E. Alpaca-LoRA: Instruct-tune LLaMA on consumer hardware. <https://github.com/tloen/alpaca-lora>, 2023.

Wang, Y., Ivison, H., Dasigi, P., Hessel, J., Khot, T., Chandu, K. R., Wadden, D., MacMillan, K., Smith, N. A., Beltagy, I., and Hajishirzi, H. How far can camels go? Exploring the state of instruction tuning on open resources. *arXiv preprint arXiv:2306.04751*, 2023.

A. SFT vs LoRA Visualization

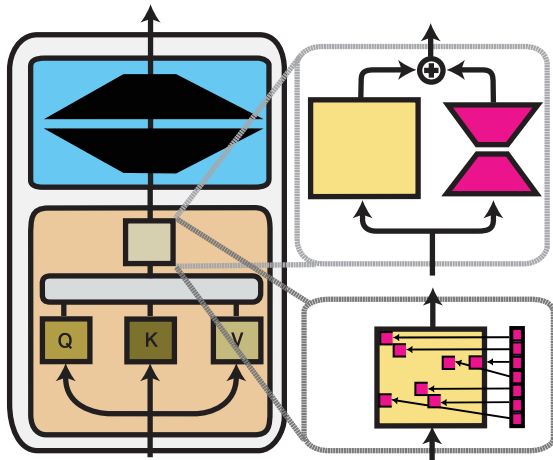


Figure 3. SFT (lower right) versus LoRA (upper right) applied to a linear layer (the output projection of self-attention) of a Transformer block.

B. Evaluation Setup

Following Wang et al. (2023) and Ivison et al. (2023), we evaluate the instruction-tuned LLMs on a range of benchmarks to capture the following abilities:

Factuality: Massively Multitask Language Understanding (MMLU; Hendrycks et al., 2021) requires the model to pick an answer from 4 candidates and covers 57 subjects including STEM, humanities, social sciences, and other disciplines. We evaluate models in a 5-shot setting and report their accuracy.

Reasoning: We sub-sample 40 examples per task from BIG-Bench Hard (BBH; Suzgun et al., 2023), a suite of the 23 most challenging tasks from BIG-Bench. We also randomly select a subset of 200 examples from Grade School Math (GSM; Cobbe et al., 2021), a collection of math problems in linguistic form. Both benchmarks require open-ended generation. We evaluate models in a 3-shot setting with BBH and 8-shot setting with GSM, and report their exact match (EM).

Multilinguality: We choose 100 examples per language from Typologically Diverse Question Answering (TyDiQA; Clark et al., 2020), a dataset for extractive question answering in 11 languages. We follow the Gold Standard setup

where each document is guaranteed to contain the answer span. We evaluate models in a 1-shot setting and report F1.

Coding: HumanEval (Chen et al., 2021) is a dataset for synthesizing programs from docstrings. We evaluate models with a temperature of 0.1 and report their precision at 1 (P@1)⁸.

C. Training Details and Hyperparameters

To select the most important hyperparameters of the PEFT methods, we perform a hyperparameter search as detailed in Appendix D with respect to (i) the number of trainable parameters (determined by rank r in LoRA or corresponding density in SpIEL)⁹; (ii) the learning rate; (iii) weight decay strength λ for SpIEL methods. We use the found hyperparameters of each PEFT method for all fine-tuning experiments.

For SpIEL, we update the set of trainable parameters η every $S = 20$ steps, fix the initial update rate ξ to 0.2, and for SpIEL-AG, we set the length γ of the gradient estimation phase to 5 steps. Note that we have performed only minimal manual tuning on the values of S , ξ and γ due to a large number of large-scale experiments coupled with constraints on our computational budget; it is possible that other values would yield better results.

We follow Wang et al. (2023)’s choice for the remaining hyperparameters: we always train for two epochs, and apply linear learning rate decay following warmup over the first 3% of training steps. The batch size is fixed at 128 and the maximum sequence length at 2,048, with longer sequences truncated. The LoRA dropout rate is set to 0.1 and LoRA α to 16. LoRA and SpIEL are applied to all linear Transformer block layers. The pretrained parameters are stored in `bfloat16` data type, while the PEFT parameters are stored in `float32`, except for quantized training, where they are also stored in `bfloat16`.

D. Hyperparameter Search

We first performed a grid search over (i) learning rate and (ii) number of PEFT parameters (determined by rank r for LoRA and d_ϕ for SpIEL), except for (IA)³ where this number is fixed. For the SpIEL methods, we also wished to establish a good value for (iii) weight decay strength λ . Since we generally obtained a good performance with the highest tested equivalent rank of $r = 64$, and being the most highly parameterized setting this was the most likely to benefit from regularization, we searched over a range of λ values with r set to 64 and the learning rate to the best

⁸Here we differ from Wang et al. (2023) in order to reduce the variance across evaluation runs.

⁹The number of trainable parameters for (IA)³ is not tunable.

value found in the initial search.

We searched for the optimal learning rate in the range of $\{3 \times 10^{-6}, 1 \times 10^{-5}, 3 \times 10^{-5}, 1 \times 10^{-4}\}$ for LoRA and SpIEL-AG, $\{4 \times 10^{-4}, 7 \times 10^{-4}, 1 \times 10^{-3}, 2 \times 10^{-3}\}$ for SpIEL-MA (the SM3 optimizer generally benefits from higher learning rates than Adam), and $\{1 \times 10^{-5}, 3 \times 10^{-5}, 1 \times 10^{-4}, 3 \times 10^{-4}\}$ for (IA)³.

As for the number of PEFT parameters, we searched over the range $r = \{8, 16, 32, 64\}$ for LoRA and the equivalent d_ϕ for the SpIEL methods. For LLaMA2-7b, these values correspond to 0.30%, 0.59%, 1.2% and 2.3% of the total parameter count respectively, and for LLaMA2-13b, they correspond to 0.24%, 0.48%, 0.95% and 1.9%.

We searched over λ values in the range $\{0, 1, 3, 10, 30\}$ for SpIEL-AG and $\{0, 0.1, 0.3, 1, 3\}$ for SpIEL-MA (since we use higher learning rates for SpIEL-MA, a lower weight decay strength is required to have the same effect).

Each hyperparameter setting was evaluated by training on the Flan v2 subset and taking the 5-shot performance on the MMLU development set.

We present the full results of the hyperparameter search in Figure 4 and summarize the best values found for each configuration in Table 4.

Method	LLaMA2-7b			LLaMA2-13b		
	lr	r	λ	lr	r	λ
(IA) ³	3×10^{-4}	-	-	1×10^{-4}	-	-
LoRA	1×10^{-4}	64	-	3×10^{-5}	64	-
SpIEL-AG	1×10^{-4}	64	30	1×10^{-5}	64	30
SpIEL-MA	1×10^{-3}	64	0.3	4×10^{-4}	64	0
Full FT	2×10^{-5}	-	-	2×10^{-5}	-	-

Table 4. Optimal settings yielded by hyperparameter search for each PEFT method and model size.

After our main experiments, we performed some additional exploration of the drop/growth schedule, adjusting both the frequency γ of dropping/growth and the schedule $k(i, t)$ of number of parameters to drop/grow at each update. We considered drop/growth frequency in the range $\{10, 20, 40, 80\}$ steps and both our default linear schedule and the cosine schedule of Evci et al. (2020), where

$$k(i, t) = \frac{\xi}{2} \left(1 + \cos \left(\frac{t\pi}{T} \right) \right) d_{\phi^{(i)}}, \quad (11)$$

recalling that ξ is the initial update rate and T is the total number of training steps. Table 5 presents our results for SpIEL-AG when fine-tuning LLaMA2-7b on the Flan v2 subset with the other hyperparameters as shown in Table 4. We find that there is not a clear preference for a linear or cosine schedule, but that a higher update frequency of

10 might be better than the 20 steps we used in our main experiments.

Type	Schedule		Benchmark	
	Steps	MMLU	TyDiQA	
Linear	10	52.0	56.4	
	20	50.7	56.2	
	40	51.5	56.5	
	80	51.3	56.1	
Cosine	10	51.8	56.3	
	20	51.6	56.5	
	40	50.2	56.5	
	80	50.9	55.4	

Table 5. SpIEL-AG results when fine-tuning LLaMA2-7b on Flan v2 subset with various frequencies and update schedule types.

For full fine-tuning, we use the learning rate of 2×10^{-5} from Wang et al. (2023). To fit the model into a single A100, we additionally resort to activation checkpointing and paged optimization.

E. Analysis of the Backward Pass for SpIEL

Consider the forward pass when sparsely fine-tuning a linear layer. We have:

$$Y = X(W + \Delta), \quad (12)$$

where the input $X \in \mathbb{R}^{b \times d_{in}}$, the pretrained weight matrix W and its sparse delta $\Delta \in \mathbb{R}^{d_{in} \times d_{out}}$, and the output $Y \in \mathbb{R}^{b \times d_{out}}$, with b , d_{in} and d_{out} being the batch size and input and output dimensions respectively. It can be shown that

$$\frac{\partial \mathcal{L}}{\partial \Delta} = X^\top \frac{\partial \mathcal{L}}{\partial Y}. \quad (13)$$

However, we only need the entries of $\frac{\partial \mathcal{L}}{\partial \Delta}$ corresponding to the currently active indices of Δ . Let $\mathbf{r} \in \{1, 2, \dots, h\}^N$, $\mathbf{c} \in \{1, 2, \dots, w\}^N$, where h and w are the height and width of Δ respectively, denote the N active indices of Δ , i.e. (r_i, c_i) denotes the position of the i th active index in Δ . Then, if we define g_i to be the gradient of the i -th active index of Δ , we have

$$g_i = \frac{\partial \mathcal{L}}{\partial \Delta_{r_i, c_i}} \quad (14)$$

$$= \left(X^\top \frac{\partial \mathcal{L}}{\partial Y} \right)_{r_i, c_i} \quad (15)$$

$$= X_{:, r_i}^\top \left(\frac{\partial \mathcal{L}}{\partial Y} \right)_{:, c_i}. \quad (16)$$

That is, the gradient of the i -th sparse update to W is given by the dot product of the r_i -th column of X and the c_i -th column of the gradient of the output Y . We can compute the gradient of the sparse updates in this manner with bN

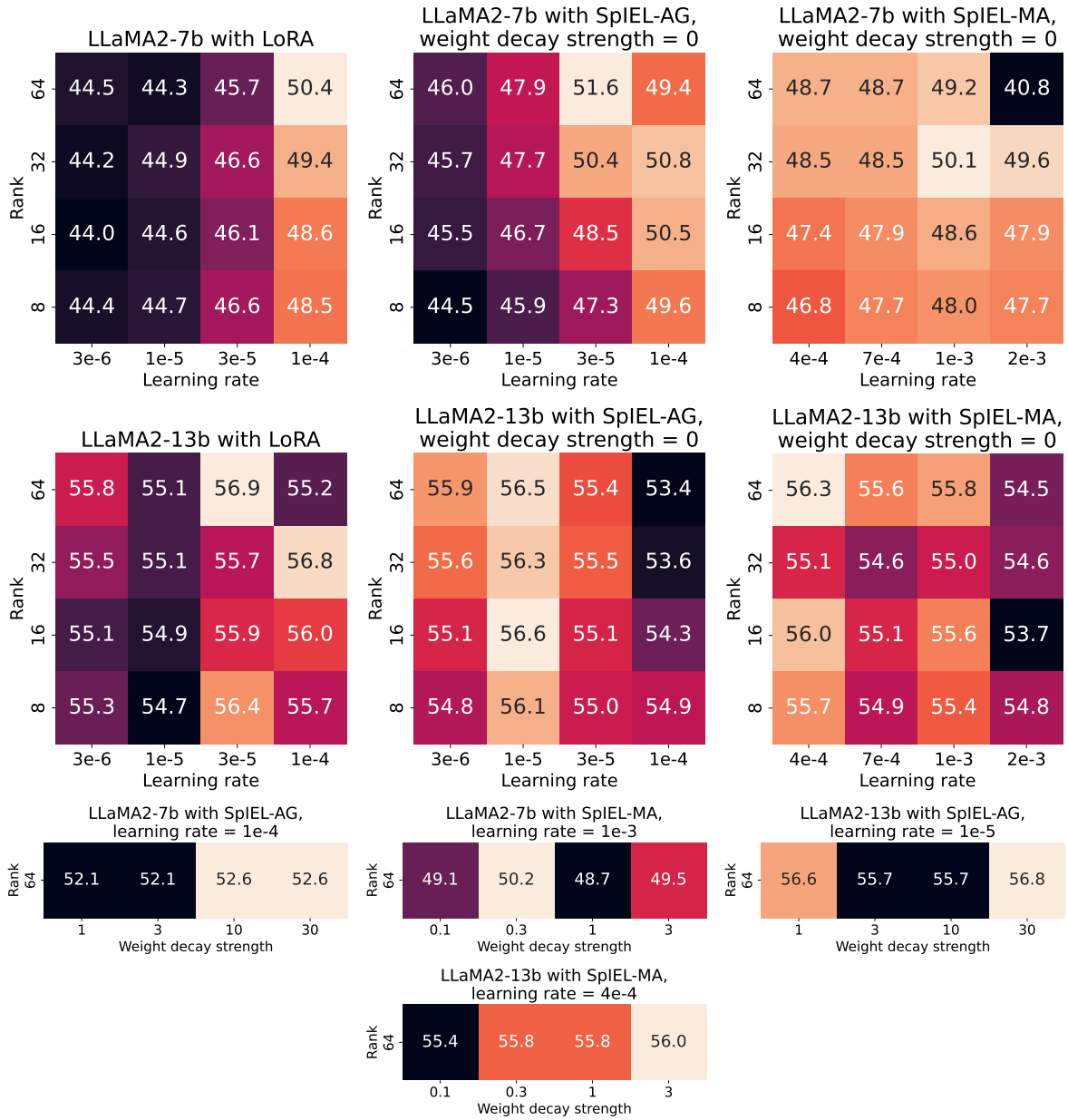


Figure 4. Hyperparameter search results.

FLOPs, which is an enormous theoretical improvement over the $bd_{\text{in}}d_{\text{out}}$ FLOPs required to naively perform the full matrix multiplication in (13) and gather the relevant indices from the result, as the SFT density $\frac{N}{d_{\text{in}}d_{\text{out}}} \ll 1$.

While calculating the sparse delta gradient in this manner entails a great reduction in FLOPs required, it is not so easy to exploit this reduction effectively on a GPU to speed the operation up. Writing an efficient CUDA kernel for this operation is ongoing work, and the speed results presented in this paper were obtained using the naive “gather from the full matrix product” method.

F. Measurement of Memory and Time Requirements

To measure the memory requirements of PEFT methods, we use PyTorch’s `set_per_process_memory_fraction` function to limit the total available GPU memory, and perform a binary search at 1 GiB granularity to find the lowest limit at which training can run successfully. For each limit we test, we run 30 steps of Flan v2 training with (equivalent) LoRA rank 64. We measure the time as the mean duration of each of these 30 steps for the lowest passing memory limit. All our experiments are run on a single A100 GPU.

We note that this may differ from the peak memory usage during (unconstrained) training, since deep learning frameworks such as PyTorch may allocate more memory than they actually require for efficiency reasons.